Evidence of mixed magnetic phases in $TbRu_2Ge_2$

A. Garnier, D. Gignoux, and D. Schmitt
Laboratoire de Magnétisme L. Néel, CNRS, B.P. 166, 38042 Grenoble Cedex 9, France

T. Shigeoka
Faculty of Science, Yamaguchi University, Yamaguchi 753, Japan
(Received 24 March 1997; revised manuscript received 24 October 1997)

In compounds with normal rare earths at the same crystallographic site, mixed magnetic phases with two distinct rare-earth magnetic states, namely, a zero moment one and another with a high moment, can be stabilized at low temperature not only in zero applied field but also in different field-induced magnetic phases of a metamagnetic process. These characteristics are observed in tetragonal $TbRu_2Ge_2$ from neutron diffraction and magnetization measurements on a single crystal. It is shown that such magnetic structures may originate from a moment instability due to the crystal field in the presence of frustrated exchange interactions. Numerical simulations using the periodic-field model allowed us to satisfactorily account for the observed properties and emphasize the crucial role played by the crystal field. [S0163-1829(98)00209-4]

I. INTRODUCTION

During the last ten years few materials with a ''mixed'' magnetic phase, where the same element lying on a unique crystallographic site has two distinct magnetic states, a nonmagnetic one and the other with a well-defined moment, have been observed. Such phases are stabilized when exchange interactions are frustrated in systems close to a magnetic instability. In RMn_2 compounds (R=rare earth), mixed phases, which occur in particular at low temperature,[1,2] involve the Mn atoms and were interpreted as resulting from the instability of band magnetism.[3] In CeSb, mixed phases, where so-called ''paramagnetic'' Ce planes coexist with magnetic Ce planes, were observed in several high-temperature phases of the complex H-T phase diagram.[4] Many studies were devoted to the understanding of this behavior. Although not completely understood, it is admitted that the original properties of this compound are related to p-f mixing that leads to a Kondo effect in presence of frustrated exchange interactions.[5,6] More recently mixed phases with normal rare earths have been suggested to exist. However one has to distinguish between systems in which the mixed phase with ''paramagnetic'' planes is induced by temperature, such as those proposed in $PrCo_2Si_2$,[7] and those in which the mixed state, with atoms in a ''zero moment'' state are, on the contrary, expected only at low temperature such as could be the case in $TbRu_2Si_2$.[8,9] In this paper we provide clear evidence for the existence of the latter situation in $TbRu_2Ge_2$ from magnetization measurements and neutron-diffraction experiments on a single crystal performed at the Laboratoire Louis Néel and at the Japan Atomic Energy Research Institute (Tokyo), respectively. Furthermore from numerical simulations, using the periodic-field model,[10] we show that crystalline electric field (CEF) effects in frustrated systems can be at the origin of the moment instability needed for such properties.

II. EXPERIMENTAL RESULTS

$TbRu_2Ge_2$ belongs to a large family of tetragonal compounds ($ThCr_2Si_2$-type structure, $I4/mmm$ space group) that present fascinating magnetic properties frequently characterized by complex phase diagrams showing several magnetic structures, depending on field and temperature. From previous magnetization and neutron-diffraction measurements the following properties of $TbRu_2Ge_2$ have been established:[11,12] (i) The huge magnetocrystalline anisotropy favors the c axis. (ii) The magnetic H-T phase diagram along the c axis is particularly complex with a large number of different phases. (iii) It orders at $T_N=37$ K in an amplitude modulated structure with propagation vector $\mathbf{Q}=(\tau,0,0)$ with $\tau=0.247$ for $T_t'<T<T_N$ and $\tau=0.233$ for $T<T_t'$, the transition temperature T_t' being 30 K. The latter value of τ does not change significantly down to low temperature. (iv) Above another transition temperature $T_t=4.3$ K, observed in susceptibility and heat capacity, two metamagnetic transitions take place in high field along c, the low-field susceptibility being rather large. (v) Below T_t, as shown in Fig. 1, three additional metamagnetic transitions appear below 1.3 T, the differential susceptibility between the steps being much smaller than above 4 K. At 2 K, saturation is reached above 3 T, the magnetization being $M_s=9.0\ \mu_B$/f.u. in 7 T, i.e., the maximum value of the Tb^{3+}

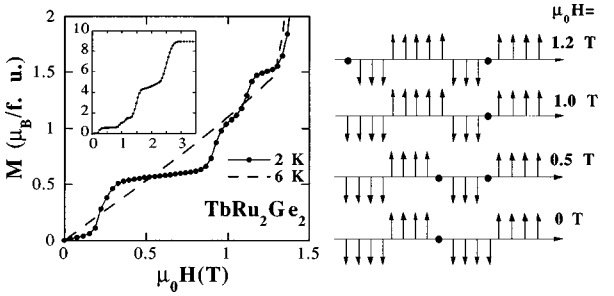

FIG. 1. Left: Low-field magnetization process in increasing field at 2 and 6 K. Right: magnetic structures at 2 K in zero field and in the first three field induced phases. Magnetization of 17 successive Tb planes perpendicular to **Q** is represented. Black dots correspond to nonmagnetic planes. Inset: M vs H at 2 K up to 3.5 T.

ion. In the following we will focus on the low-field metamagnetic transitions.

Neutron-diffraction experiments were performed on a single crystal at 2 K in different applied fields $\mu_0 H_0 = 0$, 0.5, 1, and 1.2 T, i.e., within each of the different low-field phases (phase I, II, III, and IV, respectively). As shown in Fig. 2, for all these patterns, well-defined peaks associated with high-order harmonics of the same propagation vector were observed and allowed its accurate determination: $\tau = 0.2352 \pm 0.0007$. From this value and from the multistep metamagnetic process, it can be concluded that this propagation vector corresponds to a long period commensurate structure with $\tau = 4/17 = 0.2353$. With such a value of τ, keeping in mind that the structure is body centered, there are only 17 independent sites in the magnetic cell and the description of the magnetic moment can be written as

$$\mathbf{M}(\mathbf{R}_i) = \sum_{n=-8}^{8} \mathbf{M}_{n\mathbf{Q}} \exp(2i\pi n \mathbf{Q}\mathbf{R}_i) \quad \text{with} \quad \mathbf{M}_{-n\mathbf{Q}} = \mathbf{M}^*_{n\mathbf{Q}}.$$

The intensities associated with the 8 independent Fourier components for $n = 1$ to 8 are well observed. For each field the moduli $|\mathbf{M}_{n\mathbf{Q}}|$ of these Fourier components have been deduced from the intensities after correction for the Lorentz factor and for the Tb form factor. The corresponding observed values of the $|\mathbf{M}_{n\mathbf{Q}}|/|\mathbf{M}_{\mathbf{Q}}|$ ratios are reported in Table I and plotted vs the harmonic number in Figs. 3(a)–3(d) (open squares and full lines). The statistical uncertainties of these ratios are smaller than the size of open squares in these figures. From the neutron diffraction pattern we did not extracted the $n = 0$ (or $n = 17$) Fourier component, associated with the ferromagnetic component, as the corresponding peaks fall on the nuclear peaks, leading to large uncertainties in its determination. Rather we extracted this component with good accuracy from magnetization measurements.

It is worth noting that the magnetization jumps of the first three metamagnetic transitions are approximately $M_s/17$. If one considers that, at the low temperature considered, all Tb moments are equal and have the maximum value M_s, such a jump is half that corresponding to the spin flip of one over 17 Tb moments of the magnetic cell. Knowing that $\mathbf{Q}$ does not change, the hypothesis of Tb atoms in a zero moment state, i.e., of mixed magnetic structures, within one or several low temperature phases, has to be made. One metamagnetic transition would then involve either a $0 \rightarrow M_s$ process, or a $-M_s \rightarrow 0$ process, and not a $-M_s \rightarrow M_s$ spin-flip process as generally observed in this type of material. At this stage, analysis of the neutron-diffraction patterns is needed in order to confirm this assumption and to know more precisely the magnetic structure of each phase. For each pattern we have compared the $|\mathbf{M}_{n\mathbf{Q}}|/|\mathbf{M}_{\mathbf{Q}}|$ observed ratios with those calculated for all the possible structures compatible with the observed magnetization. In each case a unique structure accounts for the experimental values. The observed ratios are compared with those of the good model in Table I and Figs. 3(a)–3(d). We also reported in these figures the ratios of one or two tested models that do not account for the experiments.

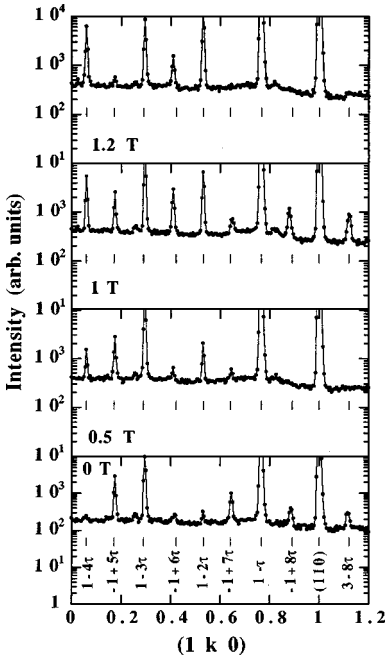

FIG. 2. **q** scans of the type (1 k 0) at 2 K in different applied fields. The values of k for the peaks corresponding to the $n\tau$ harmonics ($n = 1$ to 8) are reported in the lower panel.

Within phase I, the natural sequence of Tb planes expected for the $\tau = 4/17$ propagation vector is (4 5 4 4), where 'n' ('$\overline{n}$') stands for n successive planes with moments up (down). This structure cannot be correct for two reasons. First it would lead to a spontaneous magnetization of $Ms/17$,

TABLE I. Comparison of the observed and calculated values of the $|\mathbf{M}_{n\mathbf{Q}}|/|\mathbf{M}_{\mathbf{Q}}|$ ratios of the different harmonics within the different magnetic phases. $R = \Sigma_{n=1}^{8} \| \mathbf{M}_{n\mathbf{Q}} | (\text{obs}) - |\mathbf{M}_{n\mathbf{Q}}| (\text{cal}) | / \Sigma_{n=1}^{8} |\mathbf{M}_{n\mathbf{Q}}| (\text{obs})$. v.w.=very weak.

	$\mu_0 H = 0$ T		$\mu_0 H = 0.5$ T		$\mu_0 H = 1.0$ T		$\mu_0 H = 1.2$ T	
Harmonic	Obs.	calc.	Obs.	calc.	Obs.	calc.	Obs.	calc.
1	1	1	1	1	1	1	1	1
2	0.048	0.017	0.108	0.089	0.208	0.183	0.280	0.264
3	0.336	0.325	0.297	0.291	0.285	0.282	0.217	0.211
4	0.043	0.036	0.088	0.074	0.162	0.166	0.179	0.191
5	0.171	0.186	0.118	0.127	0.112	0.120	0.042	0.027
6	0.054	0.057	0.044	0.049	0.130	0.139	0.092	0.096
7	0.119	0.123	0.044	0.043	0.068	0.076	v.w.	0.020
8	0.087	0.084	n.o.	0.012	0.105	0.103	v.w.	0.014
	$R = 4.0\%$		$R = 3.2\%$		$R = 2.8\%$		$R = 1.7\%$	

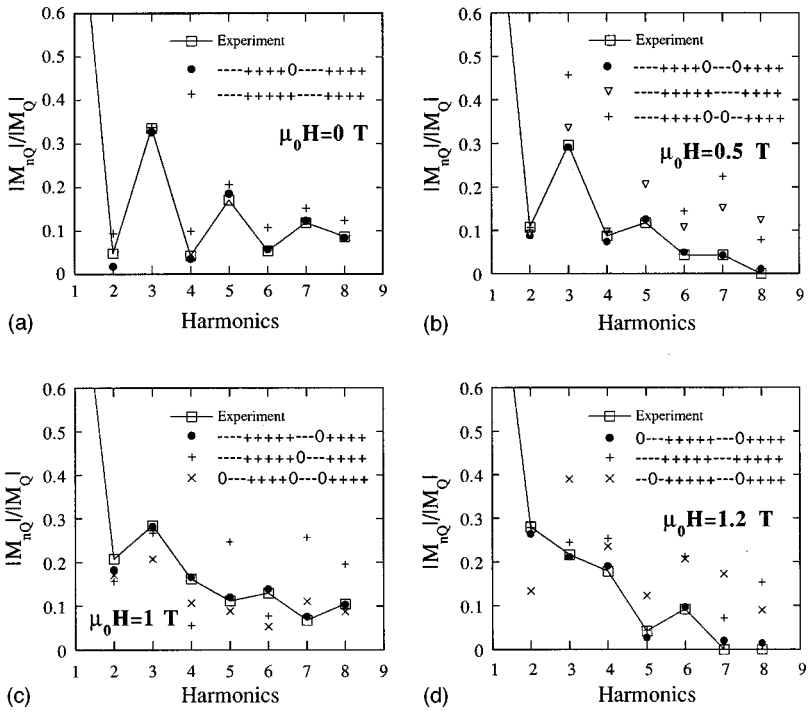

FIG. 3. Experimental and calculated Fourier components of the magnetization, normalized to $M_{\mathbf{Q}}$, at 2 K and under different applied fields. Squares are the experiment points. Black dots are the calculated points for the models that fit with the experiments. Other symbols corresponds to examples of some of the tested structures which do not agree with the experiments.

which is not observed. Second, as shown in Fig. 3(a) the associated Fourier components do not account for experimental ones [the reliability factor $R=\Sigma_{n=1}^{8}||\mathbf{M}_{n\mathbf{Q}}|(\text{obs})-|\mathbf{M}_{n\mathbf{Q}}|(\text{cal})|/\Sigma_{n=1}^{8}|\mathbf{M}_{n\mathbf{Q}}|(\text{obs})$ is 13.9]. The other solutions compatible with the absence of spontaneous magnetization have an odd number of planes, denoted '0', of Tb atoms with zero moments. As shown in Table I and in Fig. 3(a), the good solution is then obtained with the sequence (4 4 0 4 4) that leads to a reliability factor of 4.0%.

Within the first field-induced phase (phase II), in particular for a field of 0.5 T, we have considered all the possibilities for the magnetic arrangements having a magnetization of $M_s/17$. The structure that gives the best agreement ($R=3.2\%$, see Table I) with experiments is shown in Figs. 1 and 3(b). It is worth noting that the first transition involves a $-M_s\rightarrow 0$ process, and not a $0\rightarrow M_s$ process, then leading surprisingly to a magnetic arrangement with two zero moments over 17 rare-earth atoms rather than the ''natural'' one (4 5 4 4).

Within the second field-induced phase (phase III), in particular for a field of 1 T, we found the structure shown in Figs. 1 and 3(c). The reliability factor is 2.8%. This structure has only one zero moment showing that the second metamagnetic step is associated with a $0\rightarrow M_s$ process.

Finally within the third field-induced phase (phase IV), in particular for a field of 1.2 T, one has again a structure with two zero moments within the magnetic cell [see Figs. 1 and 3(d)]. The comparison between experiment and calculation leads to a reliability factor $R=1.7\%$. As for the first transition the third transition involves a $-M_s\rightarrow 0$.

It is worth noting that the solutions found for each phase are quite logical. Indeed, keeping in mind that the exchange field has the same periodicity as the magnetic arrangement (see below), the planes concerned during the metamagnetic processes are those that are near a node of the exchange field.

The result obtained from the joint analysis of magnetization and neutron diffraction is quite original. The mixed phases with normal rare earths, characterized by two moment values, i.e., 0 and M_s, are shown to exist at low temperature not only in the zero-field phase but also in the field-induced phases. The origin of such phases is certainly different from those occuring in $R\text{Mn}_2$ and CeSb. Indeed with normal rare earths the interactions driving the magnetic properties are mainly the exchange and CEF interactions and, in some compounds in particular of cubic symmetry, the quadrupolar interaction.

III. NUMERICAL SIMULATIONS AND DISCUSSION

In order to understand the origin of mixed phases in this type of uniaxial rare-earth compounds we have performed numerical simulations considering only the exchange and CEF interactions considering that the latter interaction is the same for all atoms as they belong to a unique crystallographic site whereas the exchange field can varies from one atom to the other. The approach was made in the frame of the self consistent periodic field (PF) model which has already been used to describe quite satisfactorily the magnetic properties of rare-earth antiferromagnets showing metamagnetic processes.[10] This PF model is based on an N-site Hamiltonian, N being the number of magnetic ions over one period, i.e., 17 in the present case:

$$H=\sum_{i=1}^{N} H_{\text{CEF}}(i)+\sum_{i=1}^{N} H_z(i)+\sum_{i=1}^{N} H_B(i). \qquad (1)$$

The first term is the CEF coupling. The second term is the Zeeman coupling $-\mathbf{H}\cdot\mathbf{M}(i)$ between the internal magnetic field (external field corrected for the demagnetizing field) and the $4f$ moment at site i, $\mathbf{M}(i)=-g_J\mu_B\mathbf{J}(i)$. The third term is the exchange interaction $-\mathbf{H}_{\rm ex}(i)\mathbf{M}(i)$ where the exchange field can be written, in the mean-field approximation, as

$$\mathbf{H}_{\rm ex}(i)=(g_J\mu_B)^{-2}\sum_{j\neq i}J(ij)\langle\mathbf{M}(j)\rangle$$
$$=(g_J\mu_B)^{-2}\sum_{n}\sum_{j\neq i}J(ij)M_{n\mathbf{Q}}e^{in\mathbf{Q}\cdot\mathbf{R}_j}$$
$$=(g_J\mu_B)^{-2}\sum_{n}J(n\mathbf{Q})\mathbf{M}_{n\mathbf{Q}}e^{in\mathbf{Q}\cdot\mathbf{R}_i}=\sum_{n}\mathbf{H}_{n\mathbf{Q}}e^{in\mathbf{Q}\cdot\mathbf{R}_i}, \quad (2)$$

where $\mathbf{M}_{n\mathbf{Q}}$ and $\mathbf{H}_{n\mathbf{Q}}$ are the components of the Fourier expansion of the magnetic moment and of the exchange field, which have then the same periodicity. $J(\mathbf{q})$ is the Fourier transform of the exchange interaction. The full Hamiltonian is diagonalized self-consistently for the N ions of the magnetic period, the $M_{n\mathbf{Q}}$'s obtained after diagonalization being reinjected into the initial Hamiltonian through Eq. (2). For a set of CEF and $J(n\mathbf{Q})$ parameters, it is then possible to evaluate for any field and temperature, the magnetic moment on each site and the free energy. In our case the number of CEF parameters is five whereas in principle nine $J(n\mathbf{Q})$ values are needed (in fact a least two, i.e., $J(0)$ and $J(\mathbf{Q})$, are often sufficient). Due to this large number of parameters it is a great task to determine them. Many data obtained from different types of experiments (inelastic neutron-scattering experiments for instance) are required and, in their absence, we tried to find representative parameters with the purpose of showing that mixed phases can be stabilized at 0 K.

The first step was to find CEF parameters in order to have a system with two Tb magnetic states: (i) one with a zero (or weak) moment below a threshold field and (ii) the other with a high moment above this field. This arises when the ground state is a singlet and when the first excited level is rich in $J_z=|\pm J\rangle$ Moreover the components of these levels are such as the effective field acting on the Tb ions must lead to a crossing between the two lowest levels. A set of parameters was found that gives the calculated variation of the Tb moment as a function of the effective field reported in Fig. 4. Among these parameters, reported in the caption of this figure, the second-order one is close to the value that can be deduced directly from the shift at 300 K between the reciprocal paramagnetic susceptibilities measured along and perpendicular to the fourfold axis.[12] As a second step a set of exchange parameters, namely, $J(0)=-30$ K, $J(\mathbf{Q})=25$ K, $J(2\mathbf{Q})=15$ K, and $J(3\mathbf{Q})=15$ K, was found that gives the metamagnetic process and the structures corresponding to the steps reported in Fig. 5. The main characteristics of the simulation are the followings: (i) The zero field structure (phase I) is the same as that observed (ii) The amplitude of the first step is equal to $M_s/17$ as observed whereas that of the second step reaches $2M_s/17$. (iii) The first induced phase (phase II) contains only Tb magnetic planes whereas the second induced structure (phase III) is the same as the third induced experimental one. (iv) Considering the slope of M vs H within each phase: it is zero within phase II whereas it is nonzero within phases I and III, being two times larger within phase III than within phase I. This can be understood from the variation of M vs H at 0 K shown in Fig. 4 and considering that there is zero, one and two Tb atoms with zero moment out of 17 within phases II, I, and III, respectively. Within phase I the slope corresponds to the low-field susceptibility on the site with weak moment, whereas within phase III it corresponds to the low-field susceptibility on the *two* sites with weak moments. In principle, this feature could be a good way to deduce, from the experimental variation of M vs H, the nature of each phase, i.e., mixed or not mixed and if mixed the number of atoms with zero moment. Unfortunately except for phase II, the field range of the other phases is rather narrow and the observed slope is strongly modified by the rounded effects that occur when approaching the transition fields.

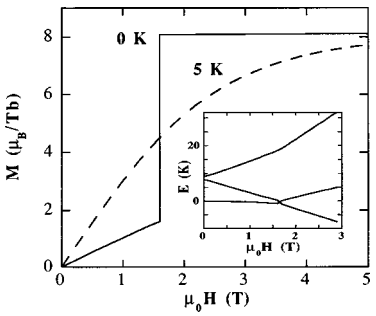

FIG. 4. Calculated terbium moment, at $T=0$ and 5 K, as a function of the effective field for the following CEF parameters: $V_2^0=798$ K, $V_4^0=432$ K, $V_4^4=1643$ K, $V_6^0=514$ K, and $V_6^4=-4900$ K. Inset: field dependence of the three lowest energy levels of Tb^{3+}.

The main features of the experimental characteristics are then well reproduced, although some details are different due to the fact that the parameters are certainly not perfect. In conclusion, numerical simulations clearly show that mixed phases, as they are observed in $TbRu_2Ge_2$, originate from CEF effects in a system where exchange interactions are frustrated. The existence of a nonmagnetic CEF singlet ground state is not enough for mixed states to be observed; the first excited state must be strongly magnetic and not too

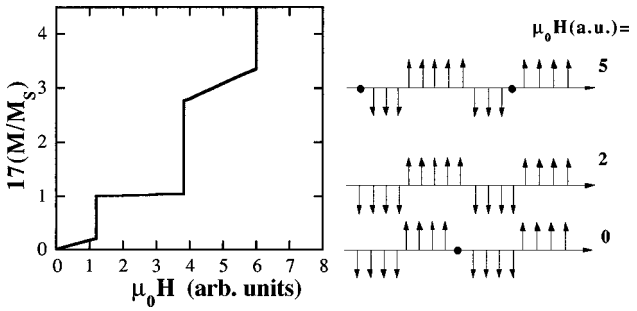

FIG. 5. Numerical simulation at 0 K using the PF model. Left: Low-field magnetization process in increasing field. Right: magnetic structures in zero field and in each of the field induced phases. Magnetization of 17 successive Tb planes perpendicular to **Q** is represented. Black dots correspond to nonmagnetic planes.

far above, and a crossing between the two lowest energy states must occur under the effective field (see insert of Fig. 4). The simulation shows that such mixed phases can be stabilized only at very low temperature. As soon as temperature increases the Tb moment varies continuously with the effective field as shown in Fig. 4 for $T=5$ K. Between 0 and 5 K there is a transition from a mixed phase, in which a node of the modulation of the exchange field falls on the 0 moment Tb plane, toward an amplitude-modulated structure in which no node of the exchange field falls on a Tb plane. The low-field metamagnetic behavior is replaced by a linear variation with a high susceptibility. This is in agreement with the observed transition temperature at 4 K and with the low-field magnetization process observed above this temperature, in particular at 6 K as shown in Fig. 1. One can wonder what is the nature of the phase transition (first, second order, or other type) below 5 K as it is characterized by a phase slip of the exchange field. This point remains to be clarified, taking into account the unusual broadness of the specific-heat peak observed at 4.3 K.

The phase diagrams of $TbRu_2Ge_2$ and $TbRu_2Si_2$ are very similar.[12] In the latter, at low temperature, the zero-field phase and the five first field-induced phases have the same propagation vector $\mathbf{Q}=(3/13,0,0)$ and the amplitude of each step is equal to $M_s/26$ (indeed, due to the body-centered structure, the magnetic cell contains 26 Tb atoms and a step associated with a $-M_s \rightarrow 0$ or $0 \rightarrow M_s$ process has a $M_s/26$ amplitude). Therefore from the present study and as suggested previously,[8,9] mixed phases certainly exist in the Si-based compound. As the magnetic cell contains an even number of Tb atoms, the zero field phase is likely not mixed whereas the first induced phase should be mixed. The transition observed at $T_t=5$ K in the Si-based compound likely has the same origin as in the Ge compound. This is in contradiction with the interpretation proposed for the heat-capacity anomaly at T_t in $TbRu_2Si_2$ that considered that the low-field antiferromagnetic structure has become a mixed phase with one out of the thirteen Tb planes paramagnetic, whereas the others have the same maximum value.[13]

$DyRu_2Si_2$ and $DyRu_2Ge_2$ exhibit magnetic phase diagrams rather similar to those of the Tb-based compounds,[14,15] and the possibility of mixed phases has been invoked.[16] This is rather surprising for a Kramer's ion in which singlet CEF levels cannot exist. However, if the CEF would lead to a low (instead of zero) magnetic state for a low effective field, the free energy of the system could be smaller when a node of the exchange field falls on a Dy plane, which is then nonmagnetic, than when no node falls on a Dy plane, as is the case for an antiphase structure with all moments equal.

[1] P. J. Brown, B. Ouladdiaf, R. Ballou, J. Déportes, and A. S. Markosyan, J. Phys.: Condens. Matter **4**, 1103 (1992).

[2] C. Ritter, S. H. Kilcoyne, and R. Cywinski, J. Phys.: Condens. Matter **3**, 727 (1991).

[3] R. Ballou, C. Lacroix, and M. D. Nunez-Regueiro, Phys. Rev. Lett. **66**, 1910 (1991).

[4] J. Rossat-Mignod, J. M. Effantin, P. Burlet, T. Chattopadhyay, L. P. Regnault, H. Bartholin, C. Vettier, O. Vogt, D. Ravot, and J. C. Achart, J. Magn. Magn. Mater. **52**, 111 (1985).

[5] T. Kasuya, Y. S. Kwon, T. Suzuki, K. Nakanishi, F. Ishiyama, and K. Takegahara, J. Magn. Magn. Mater. **90-91**, 389 (1990).

[6] T. Kasuya, A. Yanase, and K. Okuda, Physica B **186-188**, 9 (1993).

[7] K. Takeda, K. Konishi, H. Deguchi, N. Iwata, and T. Shigeoka, J. Phys. Soc. Jpn. **60**, 2538 (1991).

[8] T. Shigeoka, N. Iwata, A. Garnier, D. Gignoux, D. Schmitt, and F. Y. Zhang, J. Magn. Magn. Mater. **140-144**, 901 (1995).

[9] T. Shigeoka, M. Eguchi, S. Kawano, and N. Iwata, Physica B **213&214**, 315 (1995).

[10] A. R. Ball, D. Gignoux, D. Schmitt, and F. Y. Zhang, Phys. Rev. B **47**, 11 887 (1993).

[11] J. K. Yakinthos and E. Roudaut, J. Phys. (Paris) **47**, 1239 (1986).

[12] A. Garnier, D. Gignoux, D. Schmitt, and T. Shigeoka, Physica B **212**, 343 (1995).

[13] M. A. Salgueiro da Silva, J. B. Sousa, B. Chevalier, J. Etourneau, E. Gmelin, and W. Schnelle, Phys. Rev. B **52**, 12 849 (1995).

[14] B. Andreani, G. L. F. Fraga, A. Garnier, D. Gignoux, D. Maurin, D. Schmitt, and T. Shigeoka, J. Phys.: Condens. Matter **7**, 1889 (1995).

[15] M. Bouvier, G. L. F. Fraga, A. Garnier, D. Gignoux, D. Schmitt, and T. Shigeoka, Europhys. Lett. **33**, 647 (1996).

[16] N. Iwata, T. Shigeoka, Y. Matsuzaki, S. Kawano, and S. Mitani, Physica B **213&214**, 309 (1995).